Resonance acoustic-phonon spectroscopy for studying elasticity of ultrathin films

Cite as: Appl. Phys. Lett. **90**, 191906 (2007); https://doi.org/10.1063/1.2737819
Submitted: 07 March 2007 . Accepted: 13 April 2007 . Published Online: 08 May 2007

H. Ogi, M. Fujii, N. Nakamura, T. Shagawa, and M. Hirao

Resonance acoustic-phonon spectroscopy for studying elasticity of ultrathin films

H. Ogi,[a] M. Fujii, N. Nakamura, T. Shagawa, and M. Hirao
Graduate School of Engineering Science, Osaka University, Toyonaka, Osaka 560-8531, Japan

(Received 7 March 2007; accepted 13 April 2007; published online 8 May 2007)

Ultrahigh-frequency phonon resonances were excited in ultrathin films (~5 nm) by femtosecond light pulses, and their resonance frequencies were measured to determine the through-thickness elastic constants. The studied materials were Pt and Fe. The elastic stiffness increases with decreasing film thickness for both materials, whereas the normal strain showed opposite thickness behavior. Analysis of the wave propagation using the third-order elastic constants explained these trends. © *2007 American Institute of Physics*. [DOI: 10.1063/1.2737819]

Elastic constants of thin films are required for designing acoustic devices such as surface-acoustic-wave filters. They also help evaluate thin-film reliability affected by elastic softening and elastic anisotropy, which are caused by defects, including oriented nanocracks,[1] incohesive-bond regions,[2] and precipitates at grain boundaries.[3] In condensed-matter physics, thin-film elastic constants especially deserve study because of their extreme deformation, where the magnitude of the elastic strain can reach $\sim 10^{-2}$, which never occurs in bulk materials because of movable dislocations. Such extreme strain fields may change the elastic constants from their unstrained bulk values; this reflects an anharmonic interatomic potential (lattice anharmonicity). Therefore, the elastic constants of thin films have been intensively studied, and many measuring methods have been presented, including microtensile tests, microbending tests, reed-vibration method, surface-acoustic-wave method, resonant ultrasound spectroscopy, Brillouin scattering, and picosecond laser ultrasounds (PSLU), as reviewed in reference.[4] Among them, the PSLU method[5] is most promising because it is noncontacting (free from ambiguous gripping effects), and it determines the longitudinal-wave velocity directly related to one of the stiffnesses, without labyrinthine calculations and corrections. However, it requires film thickness larger than ~100 nm to separately detect the longitudinal-wave pulses, and it is inapplicable to ultrathin films ($<\sim 20$ nm), in which large residual biaxial stresses ($>\sim 1$ GPa) can occur,[6] again an attractive system for studying lattice anharmonicity.

Here, we present an advanced method for determining the ultrathin-film elastic constant using the femtosecond light pulses and x-ray total-reflectivity measurement. Thomsen *et al.*[5] first succeeded in detecting high-frequency phonon pulses by the pump-probe technique with ultrafast light pulses. The pump pulse enhances coherent acoustic phonons, which propagate in the through-thickness direction and repeat reflections within the film. The time-delayed probe pulse detects the pulse-echo signals through the photoelastic effect. Following its discovery, the PSLU method has been applied to various studies on mechanics and thermodynamics of thin films,[7–9] although few studies determined the elastic constant because of the difficulty of accurately determining the film thickness.

We note that the use of an ultrashort light pulse (~100 fs) is capable of accelerating phonon vibrations of frequencies up to ~10 THz. The ultrahigh-frequency components cannot propagate coherently for long distances because of the lossy phonon-phonon interactions. However, they can coherently resonate and remain in the ultrathin film for a short time, causing oscillations in the reflectivity response at the surface.

The studied materials were Pt and Fe. We deposited them either on (100) Si substrates or on borosilicate glass (B_2O_3–SiO_2) substrates by the magnetron-sputtering method. The deposition rates were 1.8 and 0.4 Å/s for Pt and Fe, respectively. The substrates were cleaned in the piranha solution (98% H_2SO_4:33% H_2O_2=4:1) before deposition. The base pressure was 5×10^{-6} Pa.

The film thickness must be measured accurately to determine the elastic modulus. We then used an x-ray total-reflectivity measurement.[10] The periodic intensity variation appears in the x-ray reflectivity spectrum in the low-angle region, which is caused by interference between x rays reflected at the film surface and at the film-substrate interface, and the period is governed by the film thickness. The reflectivity coefficient is theoretically calculated as a function of the incidence angle, which involves the film thickness as a parameter. A least-squares-fitting procedure was performed to inversely determine the thickness by fitting the theory to the measurement. Figure 1 shows an example of the fitted curve to the measurement. The high-angle x-ray diffraction (XRD) measurement was simultaneously performed to

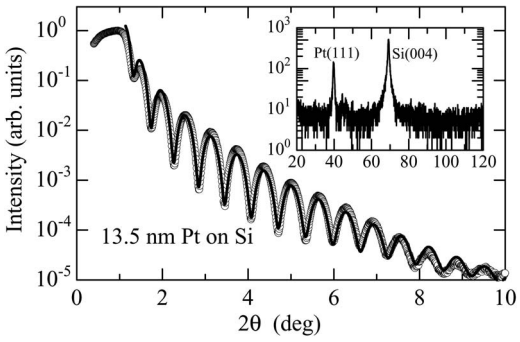

FIG. 1. X-ray total-reflectivity measurement for Pt thin film on (001) Si substrate. Open circles denote measurements and solid line denotes the fitted theoretical function. Inset shows the XRD spectrum in the high-angle region.

[a]Electronic mail: ogi@me.es.osaka-u.ac.jp

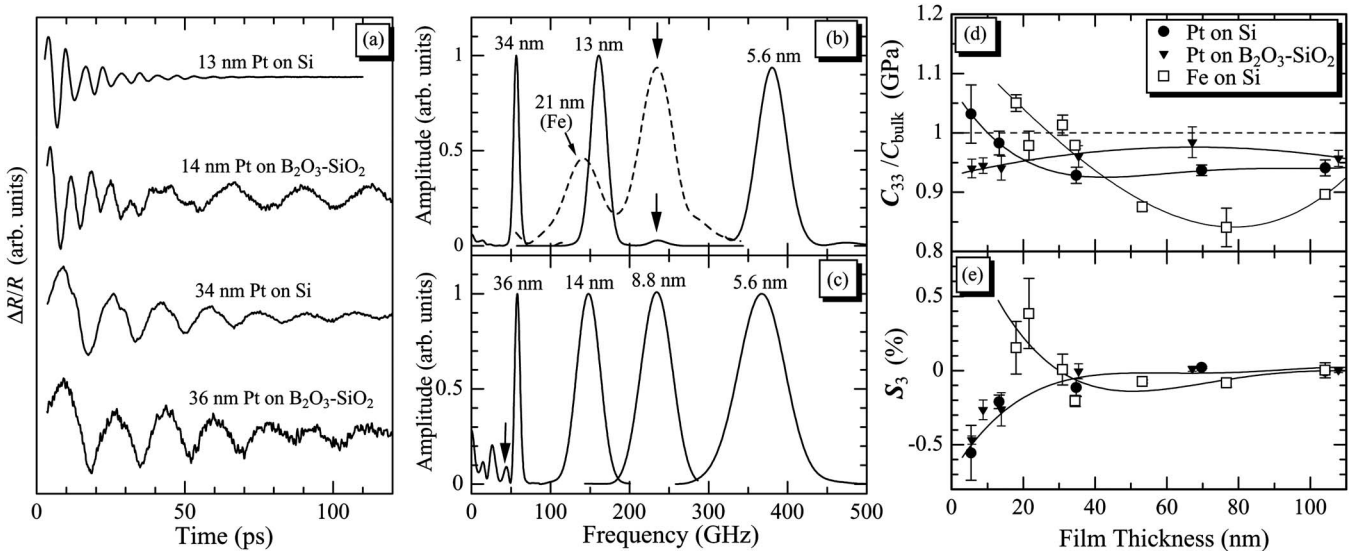

FIG. 2. (a) Time-resolved reflectivity changes observed from various thin films and their Fourier spectra for (b) Si substrate and (c) borosilicate-glass substrate. Vertical arrows indicate the Brillouin oscillations from the substrates. (d) Thickness dependence of the out-of-plane modulus and (e) that of the out-of-plane strain for Pt and Fe thin films.

evaluate the texture and the out-of-plane strain. The XRD spectra indicated strong (111) texture for Pt and strong (110) texture for Fe; diffraction peaks from other planes were negligible, as shown in the inset in Fig. 1. Therefore, we considered the complete (111) and (110) textured films for Pt and Fe, respectively. We evaluated the normal strain S_3 relatively using the thickest specimens as references because the value of the plane distance determined only by a single low-angle peak may be affected by the measurement condition.

A mode-locked Ti:sapphire pulsed laser with a wavelength of 800 nm and duration of 100 fs was focused onto the film surface after the amplitude modulation as the pump pulse. The spot diameter and average power of the pump pulse on the specimen surface were 50 μm and 20 mW, respectively. The frequency-doubled (wavelength: 400 nm) branched probe pulse was perpendicularly focused on the specimen surface with a time delay. The reflected probe pulse entered into a balanced photodetector together with the reference beam to detect the relative change of reflectivity. Further details appear in the supplemental document.[11]

Figure 2 shows the typical responses of the reflectivity variation ΔR and the corresponding Fourier spectra. For ultrathin films, we observed two kinds of oscillations [Fig. 2(a)]. The first oscillation appears just after the excitation and the second oscillation follows with lower attenuation. The second oscillation is identified as the Brillouin oscillation, caused by the interference between the light beams reflected at the substrate surface and diffracted by the acoustic waves propagating into the substrate.[12] This oscillation frequency is given by $2nv/\lambda$, where n, v, and λ denote the refractive index in the substrate, the sound velocity in the substrate, and the wavelength of the light. Taking standard handbook values, we calculate the oscillation frequencies to be 235 and 42 GHz for Si and borosilicate-glass substrates, respectively. These values agree with those observed in the spectra in Figs. 2(b) and 2(c).

The first oscillation is considered to arise from local resonances of acoustic phonons. Acoustic-phonon resonance frequencies in a monolayer film are given by $f_m = m\sqrt{C_{33}/\rho}/(2d)$ when the acoustic impedance of the film is larger than that of the substrate. C_{33} and ρ are the through-thickness longitudinal-wave modulus and the mass density of the film, and d is the film thickness. m denotes the mode index number. The resonance spectrum of Fe films was much broader [Fig. 2(b)] because the smaller acoustic-impedance mismatch between Fe and Si allowed larger energy leakage into the substrate. Using the bulk mass density and the fundamental resonance frequency (f_1), we determined the elastic modulus C_{33}. For thicker films ($d>70$ nm), separate longitudinal-wave pulses were detected, and we determined the modulus by measuring the round-trip time.

Figures 2(d) and 2(e) show thickness dependences of C_{33} and the normal strain S_3. We normalized C_{33} by the bulk values C_{bulk}, the longitudinal-wave moduli along the $\langle 111 \rangle$ and $\langle 110 \rangle$ directions for Pt and Fe, respectively; they are the maximum possible values of the longitudinal-wave modulus. First, we emphasize that ultrathin Pt films ($d<20$ nm) deposited on the borosilicate glass were significantly softer than those on the Si substrate. Resonant spectra in Fig. 2 obviously show broader peaks for ultrathin films on the glass substrate, regardless of the fact that the acoustic-impedance mismatch between Pt and the glass is larger than that between Pt and Si. Also, the x-ray total-reflectivity measurement revealed that the surface roughness of the ultrathin films on the glass substrate was larger by 30%. These observations indicate that the ultrathin films on the glass substrate are more dissipative and defective than those on the Si substrate. The lower strength of the glass may cause local failure due to the huge intrinsic stress of ultrathin films. This is an important observation, and we can thus evaluate the reliability of the ultrathin films through the elastic constants.

Next, we discuss the elastic modulus behavior of films on the Si substrate. A similar trend was observed for Pt and Fe: C_{33} increases as the thickness decreases. But, the thickness dependence of S_3 appears to be opposite for Pt and Fe. There are many mechanisms for softening of thin films, including defects as described, incohesive bonds, imperfect texture, remaining amorphous phase, interfacial effect,[7] and so on; identification of the exact cause is difficult. However, explanation of the stiffened films will be made possible by

the lattice anharmonicity. Sound-velocity changes caused by the elastic-strain field are expressed in terms of higher-order elastic constants.[13] Considering up to third-order elastic constants, we can explain the relationship between the modulus and strain behaviors in Fig. 2. In the case of small-amplitude waves in a homogeneously deformed material, the propagation condition is expressed by $\rho_0 W^2 U_i = w_{ij} U_j$, where ρ_0, W, and U_i denote the mass density at the unstrained state, the sound velocity, and the displacement. $\rho_0 W^2$ corresponds to the governing elastic constants, and they are eigenvalues of the second-rank tensor w_{ij} given by

$$w_{ij} = N_k N_l [\delta_{ij} \tilde{t}_{kl} + (\delta_{jm} + 2\eta_{jm}) \tilde{c}_{ikml}]. \quad (1)$$

Here, $\tilde{t}_{ij} = c^0_{ijkl}\eta_{kl} + (1/2) C_{ijklmn}\eta_{kl}\eta_{mn}$ and $\tilde{c}_{ijkl} = c^0_{ijkl} + C_{ijklmn}\eta_{mn}$, where c^0_{ijkl} and C_{ijklmn} are the unstrained-state second-order elastic constants and the third-order elastic constants (TOE). N_i is the eigenvector, which is along the propagation direction. η_{ij} denote the homogeneous Lagrangian strains. Thus, using the reported values of c^0_{ijkl} and C_{ijklmn},[14] we calculated the change of the elastic constants in the presence of the biaxial strain field of the films.[11]

The results yielded opposite sign of the sensitivity: $(dC^{\mathrm{Pt}}_{\langle 111\rangle}/dS_3)/C^{\mathrm{Pt}}_{\langle 111\rangle} = -5.52$ and $(dC^{\mathrm{Fe}}_{\langle 110\rangle}/dS_3)/C^{\mathrm{Fe}}_{\langle 110\rangle} = 2.42$. Therefore, the opposite thickness behavior of S_3 should cause similar behavior in C_{33}, which agrees with observation. The normal strains of the ultrathin films are larger in magnitude by about 0.5% than those of the thickest films, and according to the theory above, those strains yield 3% and 1% increases of C_{33} in Pt and Fe films, respectively. These values are, however, significantly smaller than the observed changes. One possible reason is that the reported values of TOEs are smaller in magnitude than the true values. This may occur because the determination of TOEs is never straightforward and easily provides underestimated values because of dislocation movements.[15]

In conclusion, we developed an acoustic-phonon-resonance spectroscopy method for accurately measuring the through-thickness elastic constant C_{33} of ultrathin films. The moduli of ultrathin Pt and Fe films increase with the decrease of film thickness and they exceed the possible maxima of their bulk values. This trend was explained by considering the third-order elastic constants, which enter the problem because of the large strains in the ultrathin films.

[1] H. Ogi, G. Shimoike, M. Hirao, K. Takashima, and Y. Higo, J. Appl. Phys. **91**, 4857 (2002).
[2] N. Nakamura, H. Ogi, and M. Hirao, Acta Mater. **52**, 765 (2004).
[3] H. Ogi, N. Nakamura, H. Tanei, R. Ikeda, M. Hirao, and M. Takemoto, Appl. Phys. Lett. **86**, 231904 (2005).
[4] H. Ogi, N. Nakamura, H. Tanei, and M. Hirao, Mater. Res. Soc. Symp. Proc. **875**, 3 (2005).
[5] C. Thomsen, H. Grahn, H. Maris, and J. Tauc, Phys. Rev. B **34**, 4129 (1986).
[6] J. Floro, S. Hearne, J. Hunter, P. Kotula, E. Chason, S. Seel, and C. Thompson, J. Appl. Phys. **89**, 4886 (2001).
[7] B. Clemens and G. Eesley, Phys. Rev. Lett. **61**, 2356 (1988).
[8] H. Grahn, H. Maris, J. Tauc, and K. Hatton, Appl. Phys. Lett. **53**, 2281 (1988).
[9] B. Perrin, B. Bonello, J.-C. Jeannet, and E. Romatet, Physica B **219-220**, 681 (1996).
[10] L. Parratt, Phys. Rev. **95**, 359 (1954).
[11] See EPAPS Document No. E-APPLAB-90-064719 for details of optics and calculations of the modulus change caused by the axial strain field. This document can be reached via a direct link in the online article's HTML reference section or via the EPAPS homepage (http://www.aip.org/pubservs/epaps.html).
[12] A. Devos and R. Côte, Phys. Rev. B **70**, 125208 (2004).
[13] R. Thurston and K. Brugger, Phys. Rev. **133**, A6 (1964).
[14] c^0_{ijkl} and C_{ijklmn} of Fe are from references given by H. Ledbetter and S. Kim, in *Elastic Grüneisen Parameters of Cubic Elements and Compounds*, Handbook of Elastic Properties of Solids, Liquids, and Gases Vol. II, edited by M. Levy, H. Bass, and R. Stern (Academic, San Diego, 2001), p. 97; C_{ijklmn} of Pt are from S. Mathur and P. Gupta, Acustica **31**, 114 (1974).
[15] K. Salama and G. Alers, Phys. Rev. **161**, 673 (1967).